STRUCTURAL AND ELECTROCHEMICAL PROPERTIES OF AG_xSNO_{1-x}/G $(0.3 \leq x \leq 0.4)$ COMPOSITE ELECTRODES

M. Alpha., U.E. Uno., Isah K.U., Ahmadu U.

Department of Physics, Federal University of Technology Minna, P.M.B 65, Minna, Nigeria

ABSTRACT: *The electrochemical performance of Ag_xSnO_{1-x}/G composite ($0.3 \leq x \leq 0.4$) as an electrode material was investigated for supercapacitor application. The reduce graphene oxide (G) was synthesized using an improved modified Hummer's method and the composites electrode material was synthesized with a hydrothermal reduction method. The introduction of Ag_xSnO_{1-x} ($0.3 \leq x \leq 0.4$) material into the network of the reduce graphene oxide enhances the kinetic for both charge transfer and ion transport throughout the composite electrode. The composite was characterized by Raman, SEM and XRD which reveals the morphology and structural properties. The Electrochemical properties were investigated using cyclic voltammetry and electrochemical impedance spectroscopy analysis. The electrode Ag_xSnO_{1-x} ($x = 0.4$) gives the specific capacitance of 123.1 F/g, energy density of 30.9 Wh/kg, and power density of 541.1 W/kg after one cycle. After 1000 cycles CV test, it gives the capacitance efficiency of 95.4 % capacitance retention. The composites showed greatly improved cycling stability and demonstrated positive synergistic effect between Ag_xSnO_{1-x} ($0.3 \leq x \leq 0.4$) material and the reduce graphene oxide as composite electrode to meet the requirement for high energy and power density.*

KEYWORDS: Electrode, Supercapacitance, Composite

INTRODUCTION

To develop an advanced supercapacitor, low cost and high efficiency are very essential. Based on these prerequisites, much interest has been focused on the electrode material to improve both energy density and power density [1-3]. The preparation of composite material with high surface area by introduction of metal oxide into the network of reduce graphene oxide is one of the efficient approach for improving the performance of the electrode material [4-5]. Carbonaceous substances indicate best physical and chemical properties while the polymers with conductivity properties present high pseudo capacitance, low cost, conductivity, best energy density. However, EDLCs have the best pore-size and surface area. Transition metal oxides materials as pseudocapacitors can present excellent specific capacitance and energy storage density [6]. Carbon materials have been applied as framework to support Ag-ion host materials, such as phosphorous [7], Sn-based compounds [8], in order to increase the electronic conductivity of electrode materials during charge/discharge processes. Graphene has been widely used as effective building blocks for these purposes, owing to its high electronic conductivity, two-dimensional structure with high surface area, and flexibility. In order to meet the demand of high energy storage, numerous efforts have been devoted to enhancing the electrochemical performance of the graphene-based composite materials based on rational material manipulations [9].

It is very important to note that among tin oxide compounds, tin dioxide (SnO_2) and tin monoxide (SnO) have attracted much attention due to their potential applications in

optoelectronic devices such as solar cells, displays, sensors, and complementary oxide-thin film transistors [10]. The existence of different oxidation states in tin ion makes it more beneficial to have non stoichiometric tin oxide phases. SnO_2 is generally an n-type semiconductor due to the existence of intrinsic defects such as oxygen deficiencies and tin interstitials, but Ag_xSnO_{1-x} exhibits p-type conductivity and relatively high hole mobility originated from the tin vacancy. From the literature concerned, most research work in the past has paid attention to SnO_2, whereas experimental reports on SnO are fewer because of its meta-stability and tendency to transform into SnO_2 at high oxygen pressures [11]. However, interest in SnO has been recently resurged because of the difficulty in obtaining high quality p-type oxide semiconductor such as p-type-doped NiO and CuO. It is believed that the p-type conductivity of SnO can be further improved by proper doping [12, 13].

In this research, the electrochemical performance of the composite electrode material was enhanced through adjustment of the electrode composition by combining reduced graphene oxide with active Ag_xSnO_{1-x}, $(0.3 \leq x \leq 0.4)$. This composite electrode gives an electrode system with high energy and power density due to the large charge surface area, high capacitance, high electrode potential and low equivalent series resistance (ESR).

Hydrothermal reduction technique is an inexpensive and direct synthesis route used to prepare simple bulk and composite materials of different nano-architectures. The hydrothermal reduction process allows for direct growth of the synthesized material on numerous substrates which enables the in-situ fabrication of advanced micro-, meso-, and macro-particulate hybrid structures [14]

Some key advantages of this technique include the ability to control and fine-tune the materials' morphology to fit the desired application and the environmentally friendly nature of closed system in which the reaction takes place.

Reversible redox process of the composite electrode in 2 M KOH electrolyte solution with respect to charging and discharging throughout the operating voltage window enhances the electrode performance. The loss of energy due to heat in each cycle is managed by easy removal due to its relatively small amount. Thus, the cycle efficiency is high. The negligibly small chemical charge transfer reaction and phase changes during charging and discharging, gives the composite material good cyclability and durability

Pure graphene can be modified by oxygen or other heteroatoms to show increased electrochemical capacitance. Such a gain is attributed to the redox activity enabled by the hetero atoms, known as pseudocapacitance which is the same as or comparable with the common capacitive behaviour that is featured by rectangular cyclic voltammograms [15]. It is commonly considered to result from electrode surface confined electron transfer reactions and hence is Faradaic in nature [16]. However, the rectangular CVs of pseudocapacitance are in contrast to those peak-shaped CVs that can be predicted from the Nernst Law for single or multiple electron transfer reactions in surface confined battery-type materials. The differences between the Faradaic capacitive and Faradaic Nernstian electrode reactions are claimed to result from, respectively, the transfer of partially delocalised and localised valence electrons, although no theoretically justified explanation has yet been reported [17]. However, current studies on laboratory made graphene oxides (GOs) have not yet been revealed well-defined atomic structures which bring difficulties to resolve the electronic structures. Further, oxygen in GOs is known to only exist in a few forms [18].

Experiment

Methods

The Reduced Graphene Oxide was synthesis using modified Hummer's methods and the composite material using hydrothermal reduction method at Advanced Chemistry Laboratory, Sheda Science and Technology Complex (SHESTCO) Abuja, Nigeria. All apparatus for the synthesis were washed with distilled water and then dried in an electric oven at 60 ^{0}C for 30 mins before used.

Synthesis of Reduced Graphene Oxide (G)

5g of graphite, 2.5 g of $NaNO_3$ and 115 mL H_2SO_4, (98%) were added together and stirred for 30 min using a magnetic stirrer. The mixture was then transfer into an ice bath, then 15 g $KMnO_4$, was added slowly to mixture and maintained at below 20 ^{0}C, after the $KMnO_4$ was added, the temperature was then raise to 35 ^{0}C and stirred again for another 30 min. 230 mL of distilled water and ascorbic acid (5 mg dispersed in 10 mL of water to produce a 0.5 mg mL^{-1}) to aid reduction was then added slowly to the mixture and temperature raised to 98 ^{0}C and stirred for another 15 min. At the end of the 15 min, 400 mL distilled water and 50 mL H_2O_2 at 30 % was added to the mixture then filtered and then wash with 1 M HCl then with 100 mL DI water and we get a cake of the reduced graphene oxide and dried in an electric oven for 60 min.

Synthesis of Ag doped SnO reduced graphene oxide (Ag_xSnO_{1-x}/G) composite ($0.3 \leq x \leq 0.4$)

10 mg of the G was dispersed in 20 mL of water to produce a 0.5 mg mL^{-1} completely water dispersed G.

i. G solution (0.5 mg mL^{-1}) was mixed with 10 mL of water containing (7 mg $SnCl_2.2H_2O$ and 3 mg $AgNO_3$), ascorbic acid (5 mg dispersed in 10 mL of water to produce a 0.5 mg mL^{-1}) to aid reduction and 10 mL of ethanol to aid homogeneity for the synthesis of $Ag_{0.3}SnO_{0.7}$/G composite

ii. G solution (0.5 mg mL^{-1}) was mixed with 10 mL of water containing (6 mg $SnCl_2.2H_2O$ and 4 mg $AgNO_3$) and 10 mL of ethanol to aid homogeneity for the synthesis of $Ag_{0.4}SnO_{0.6}$/G composite.

The whole mixtures in (i. ii.) were sonicated at 60 ^{0}C for 3 h in a bath sonicator. After sonication the sample was then mixed with Polyvinylidene fluoride (PVDF) binder in a ratio 10:0.5 on a carbon paper substrate and dried in an electric oven at 60 ^{0}C for 60 min to get the composite electrode.

Electrochemical Analysis

The electrochemical analyses of the samples were carried using Cyclic Voltammetry and Electrochemical Impedance Spectroscopy (EIS) tests from a CH1604E Electrochemical Analyser, controlled by EC-Lab VlO.37 software. The CH1604E Electrochemical Analyser is an electronic instrument designed to control the potential difference (E) applied to the working electrode (WE) with a current flow (in form of either a half cell or a full cell), a reference electrode (RE) with no current and the counter electrode (CE) through which current leaves the electrolyte while measuring the potential difference between the WE and RE.

The CH1604E Electrochemical Analyser generates characteristic cyclic voltammetry curves which give us information on the possible thermodynamics of electrochemical reactions of the system. All tests in this study were carried out in a three electrode configuration. A 2 M KOH aqueous solution served as the electrolyte which provides a medium for current flow and ion interaction.

RESULTS AND DISCURSION

Results and Discussion on Structural properties

The structural properties of the composite materials were analysed using the following characterisation; the Raman analysis, XRD and SEM.

Raman analysis

Figure 1 gives the Raman spectra of the Ag_xSnO_{1-x} ($0.3 \leq x \leq 0.4$) graphene composites. In this study, Raman spectra was recorded with a high resolution Jobin-Yvon Horiba T64000 micro-Raman spectrometer equipped with a triple monochromatic system to eliminate contributions from Rayleigh scattering. The samples were excited using the 514 nm wavelength of an argon excitation laser with a power of 1.5 mW at the source. The laser focused on the sample using a 50X objective with an acquisition time of 60 - 120 s for each spectrum.
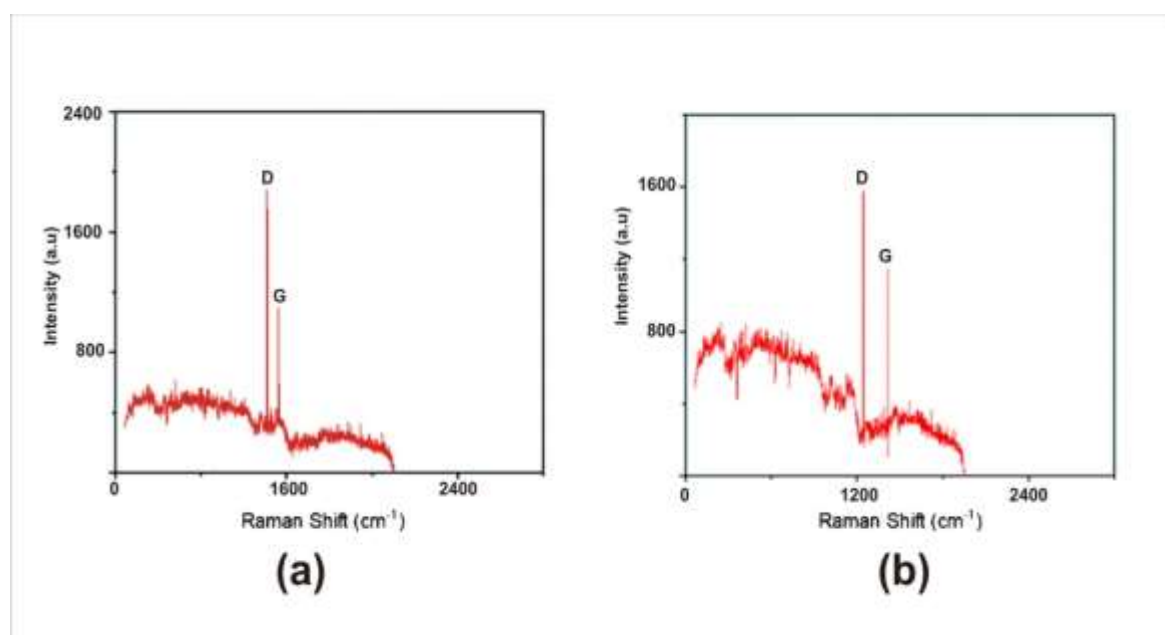

Figure 1 Raman spectra for (a) Ag_xSnO_{1-x}/G (x=0.3), (b) Ag_xSnO_{1-x}/G (x=0.4)

From figure 1, the D band is the defects and disorder mode which is due to two phonons with opposite momentum in the highest optical branch near the K point in the Brillouin zone while the G band is the sp^2-bonded vibration from carbon atoms (hexagonal lattice of graphitic material). The G and the D band are due to the bond stretching of all pairs of sp^2 atoms and the vibrating modes of the sp^2 bond [15]

From figure 1, the Raman shift for the composites give a D band spectra region at about 1348 cm^{-1} and a G band spectra region at about 1500 cm^{-1} (which is the high frequency Raman active E_{2g} mode). From figure 1 a shift of the D band intensity was observed for all the composites. This shift may have originated from structural distortion of the reduce graphene oxide [16, 17] this is as a result of the different bond distances of C–C atom and C-Ag, C-Sn atoms due to the introduction of the 3D doped metal oxide in graphene networks. The Ag dopants interact with the Sn^{4+} providing additional active sites in the composite material which results in a strong coupling between the metal species and the reduce graphene oxide, resulting in shift in the D band. The Raman shift gives the I_D/I_G intensity ratio of 1.6 for Ag_xSnO_{1-x}/G (x = 0.3) and I_D/I_G intensity ratio of 1.3 for Ag_xSnO_{1-x}/G (x = 0.4). This explains the extent of reduction of the graphene oxide. Since reduce graphene oxide is not purely sp^2 system but a highly disordered one with a significant sp^3 property, the decrease in I_D/I_G intensity ratio is due to increase in defects with increase in doping concentration. This is because there would be more sp^2 C atoms surrounding the defects and is responsible for the formation of the D band and not the defects themselves. The shift in the D band intensity may also be due to slight change in temperature during the synthesis of the composite material.

SEM Analysis

Figure 2 gives the SEM images of Ag_xSnO_{1-x}/G (x-=0.3) and Ag_xSnO_{1-x}/G (x= 0.4). The surface morphology and microstructure of all samples in this work were investigated using Phenoworld Pro X Model scanning electron microscope (SEM) operated at 2 kV in secondary electron detection mode. Samples were placed on the carbon double-sided tape attached to an aluminum substrate holder.

(a)
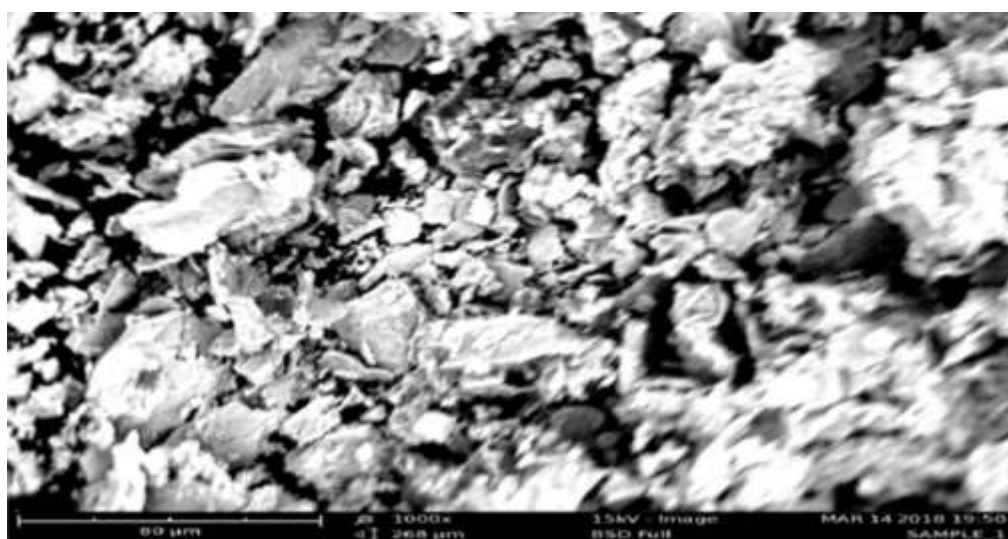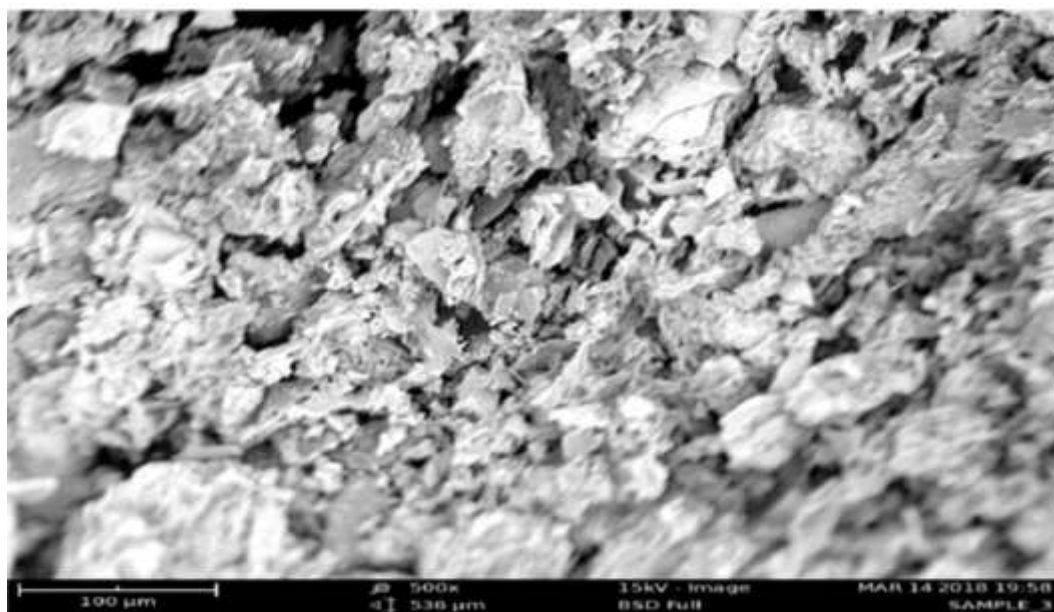
Figure 2 SEM images for (a) Ag_xSnO_{1-x}/G (x-=0.3) (b) Ag_xSnO_{1-x}/G (x= 0.4)

The SEM images in figure 2 reveals that the doped metal oxide is sandwiched chemically within the layers of the reduced graphene oxide, resulting in the formation of 3D architectural composite material and also reveals good quality dispersion. The SEM images showed relatively uniform porous surface structures for the doped metal oxide graphene composites and were observed to increase with increase in the doping concentration for the composite materials. The SEM images also indicated a slight increase in the number of grain boundaries, signifying a breakdown of the surface coalescence with increasing dopant concentration. However, since all the samples were synthesis under identical conditions, an almost similar microstructure and surface morphology was seen in all the doped metal reduce graphene electrode composites irrespective of the doping concentration.

Graphene layers interacting by means of van der Waals forces [18] and form an open pore system through which electrolyte ions can easily access the surfaces of the graphene, which facilitate the formation of electric double layers and improve the electrochemical utilization of Ag, and Sn nanoparticles into the network of the composite electrode. The doped metal oxides improve the accessibility due to their metal-cation and regular 3D dispersion in the structure of the electrode. The doped metal oxide was being used as a spacer to prevent agglomeration, and thus avoid the loss of their high active surface area which ensures high electrochemical utilisation of the reduced graphene oxide and also contribute to the total capacitance.

XRD Analysis

In this study, the crystal structures of Ag_xSnO_{1-x}/G (x = 0.3), Ag_xSnO_{1-x}/G (x = 0.4) composites was carried out using an XPERT-PRO diffractometer (PANalytical, Netherlands) with CuKá1 radiation source of wavelength 1.5406Å and operated at 35 kV and 50 mA with a scanning speed of 0.02° per step. The XRD patterns of all specimens were recorded in the 10.0° - 60.0°

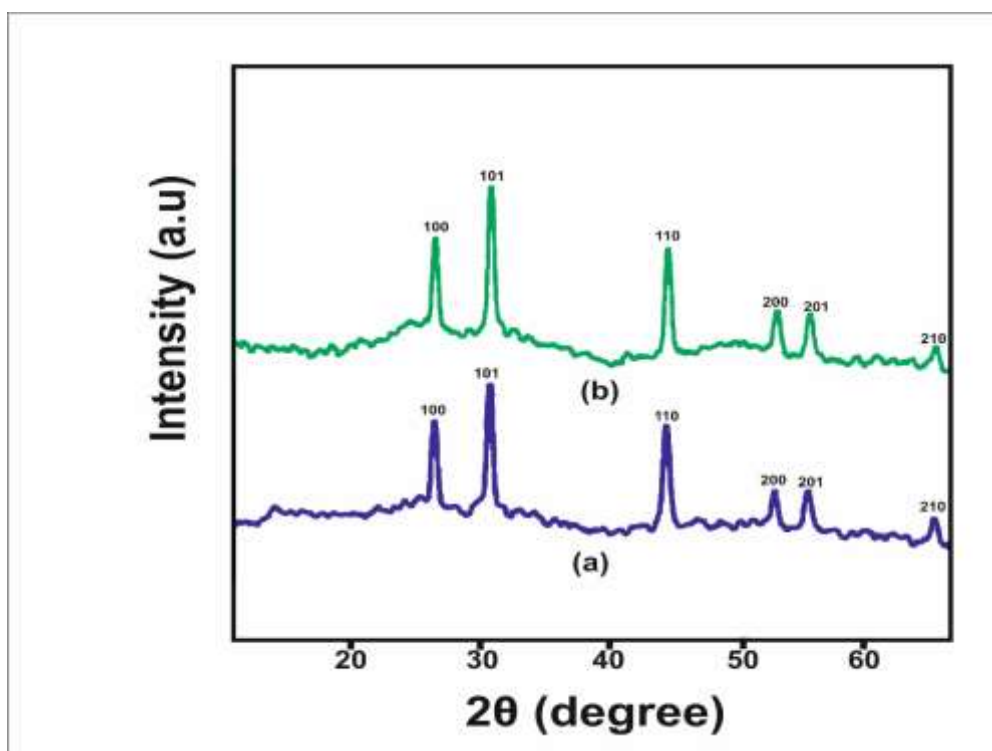2θ range with a counting time of 15.240 s per step. Figure 3 gives the XRD diffractograms of the composites.

Figure 3 XRD Diffractograms for (a) Ag$_x$SnO$_{1-x}$/G (x-=0.3) (b) Ag$_x$SnO$_{1-x}$/G (x= 0.4)

Figure 3(a) show the XRD diffractograms of the composite material Ag$_x$SnO$_{1-x}$/G (x= 0.3), with Bragg diffraction peaks at 2θ values of 25.84^0, 30.01^0, 43.06^0, 52.58^0, 55.88^0 and 66.86^0, corresponding to (100), (101), (110), (200), (201) and (210) reflection planes respectively which is well indexed to the pure tetragonal phase (JCPDS card no. 71-5324). Figure 3(b) show the XRD diffractograms of the composite material Ag$_x$SnO$_{1-x}$/G (x=0.4) with Bragg diffraction peaks at 2θ values of 25.84^0, 30.01^0, 43.06^0, 52.58^0, 55.88^0 and 66.86^0, correspond to (100), (101), (110), (200), (201) and (210) reflections planes respectively which is well indexed to the pure tetragonal phase (JCPDS card no. 71-5324).

The preferred orientations is along the peaks with the planes (100), (101) and (111) reflections and have a relatively high intensity which of course is directly proportional to the number of diffracting particles (atoms or groups of atoms) for the entire sample irrespective of the doping concentration and have tetragonal rutile-type structure. This indicates improving ordering of the reduced graphene oxide along the stacking direction due to the presence of the doped metal oxide and also due to change in electron density in the conduction band because of the introduction of active cations (Ag$^+$) in the reduced graphene oxide material. The broad peaks indicate the stacking direction comprising largely of reduced graphene oxide [19-21]. This is as a result of early crystallization. That might still be due to oxygen group insertion between the layers of the reduced graphene oxide which may cause increase interplanar distance. Particle size distribution at a size of Agglomeration may also be responsible for the unexpected reduction in the peak intensities for the Ag$_x$SnO$_{1-x}$/G electrode composites.

It is also possible that smaller particles form agglomerates that are of similar size to the primary particles of the reduced graphene oxide. In general, the reflection planes in the reduced graphene oxide sample are very poorly order along the stacking direction revealing that the reduced graphene oxide made up of largely free graphene sheet but with little of insertion of interplanar oxygen group, this agreed with [9], [17], while the reflection planes in the composite materials reveal improving ordering along the stacking direction.

Results and Discussion on Electrochemical Analysis

The electrochemical properties of the composite materials were analysed using Cyclic Voltammetry (CV) and the Electrochemical Impedance Spectroscopy (EIS) analysis.

The cyclic voltammograms from the Cyclic Voltammetry analysis for Ag_xSnO_{1-x}/G (x=0.3) and Ag_xSnO_{1-x}/G (x=0.4) at a scan rate of 100 mVs^{-1}, current density of 100 mA/g is given in figure 4. The Nyquist plot from the Electrochemical Impedance Spectroscopy analysis for Ag_xSnO_{1-x}/G (x=0.3) and Ag_xSnO_{1-x}/G (x=0.4) composites electrode materials is given in figure 5.
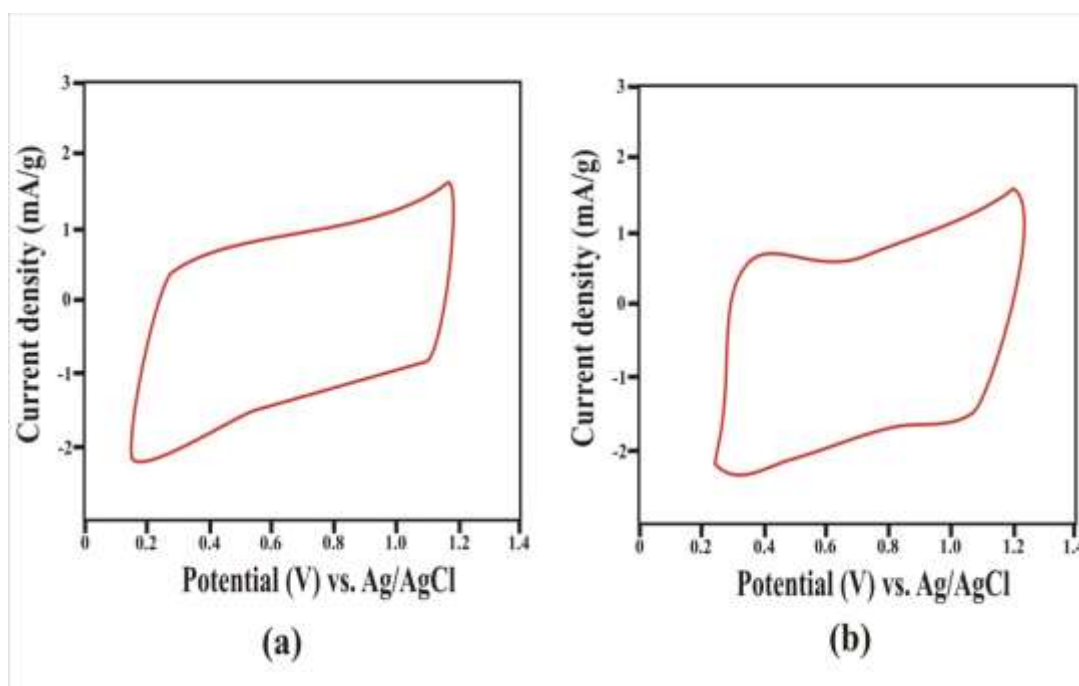
Figure 4 Cyclic Voltammogram for (a) Ag_xSnO_{1-x}/G (x-=0.3) (b) Ag_xSnO_{1-x}/G (x= 0.4)
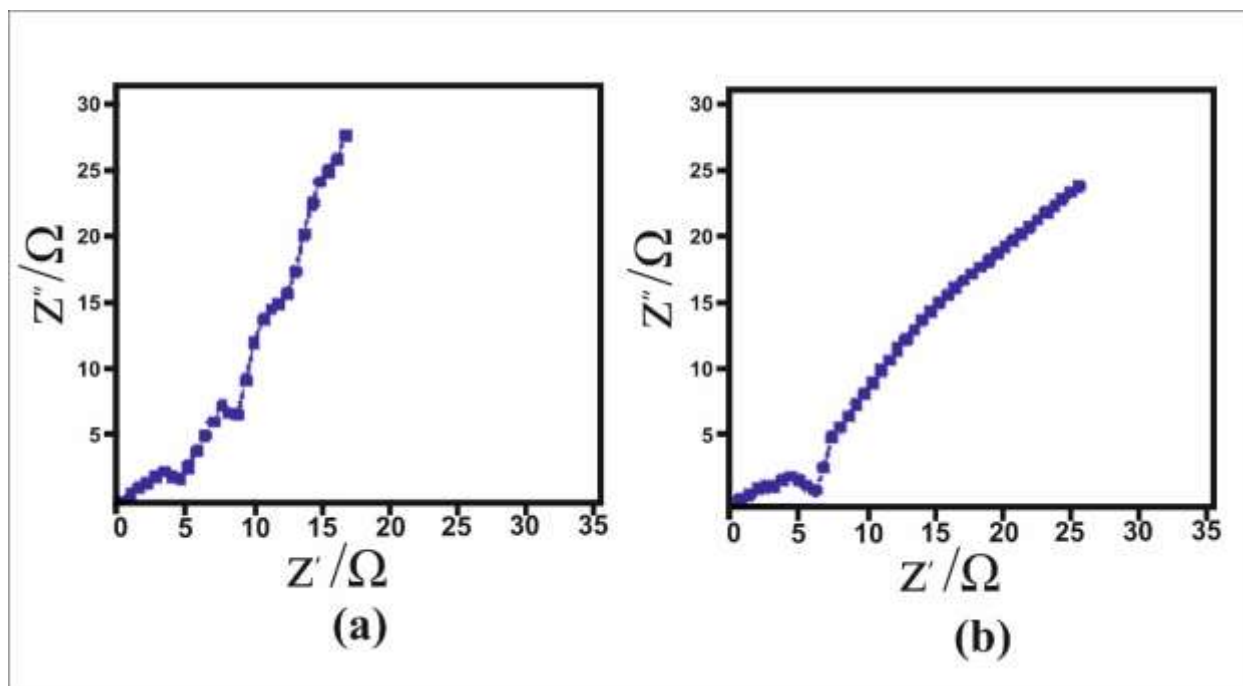
Figure 5 Nyquist plot for (a) Ag$_x$SnO$_{1-x}$/G (x-=0.3) (b) Ag$_x$SnO$_{1-x}$/G (x= 0.4)

The specific capacitance (C$_{sp}$) was calculated using the equation;

$$C_{sp} = \frac{S}{2mk(E)}$$ (1)

[22]

Where C$_{sp}$ is the specific capacitance, S is the integral charge surface area of the CV curve in (mA.V), m is the mass of the electrode material in (g), k is the scan rate in (mV/s) and E is the value of the electrode potential in (V).

The energy density (E$_D$) and power density (P$_D$) were calculated using equations

$$E_D = \frac{1}{8}C_{sp}V^2$$ (2)

Where C is the specific capacitance in F/g, V is the electrode potential in volts

The power is the energy expended per unit time and since the capacitor usually consists of the current collector, electrode and dielectric material, there will be an associated equivalent series resistance (ESR) from these extra components. As such; the associated maximum power density the cell can deliver is expressed as:

$$P_D = \frac{1}{4X(ESR)}\frac{V^2}{M}$$ (3)

Where ESR is the equivalent series resistance and M is the total mass of active material. The values of the equivalent series resistance (ESR) for the composites electrodes were obtained from the Nyquist plot in figure 5. The summary of the results from the electrochemical analysis is given in table 1.

Table 1 Summary of results from electrochemical analysis for one cycle

Composite	Mass (g)	C_{sp} (F/g)	ERS (Ω)	E_D (Wh/kg)	P_D (W/kg)
Ag_xSnO_{1-x}/G (x=0.3)	0.137	121.7	4.0	29.3	394.6
Ag_xSnO_{1-x}/G (x=0.4)	0.139	123.1	3.5	30.9	541.1

The electrochemical properties and capacitance measurement of the composite electrodes were studied using three electrode system by cyclic voltammetry (CV) and electrochemical impedance spectroscopy (EIS). The CV curves from figure 4 gives a quasi-rectangular shape due to the kinetics of electron transportation in the electrode material and the ion adsorption-desorption at the electrode and electrolyte interface and also due to the substantial contribution of pseudocapacitance to the system. From table 1, it was observed that there was increase in the energy density, power density and specific capacitance of the composites electrodes with increase in doping concentration of the cations (Ag) in the composite electrodes. This is due the expansion of the active sites when the 3D $AgxSnO1-x$, (0.3 ≤ x≤0.4) materials were introduced into the network of the reduce graphene oxide. The increase in the capacitance is due to the mixed proton-electron conductivity from the cations and the electrolyte ions. This increase in energy and power density with increase in doping concentration is also attributed to increase in charge surface area which decreases diffusion distance; this could be attributed to high Ag + diffusion coefficient, since ions diffusion is one of the most crucial processes that control the redox reaction within the electrode material [3]. The greatly enhanced specific capacitance for the composite is probably due to the synergetic effect between the reduce graphene oxide and the $AgxSnO1-x$ (0.3 ≤ x≤0.4) material. This not only effectively inhibit the stacking/agglomeration of the reduce graphene oxide but also improving the high electrochemical utilization of the composites electrodes. EIS measurement was carried within the probed frequency range of 100,000 to 0.1 Hz. It can be clearly observed that the impedance curves from the figure 5 consist of an arc and followed by a slanted line in the low frequency region. While in the high frequency region, the intercept of the semi-circle on the real axis of the Nyquist plot represent the solution equivalent series resistance which can be correlated to the Ohmic resistance of the electrolyte in the system and the charge transfer resistance between interface of the electrode materials and the electrolyte. The Warburg impedance is related to the diffusional impedance of the electrochemical system which is employed to fit the straight line at the intermediate frequency, followed by a near vertical line at the lower frequency region [21]. From table 1, a decrease in ESR for all composite with increase in doping concentration was observed. This was due to the increase in the current response with increase in doping concentration. The decrease in the value of the ESR implies; the improve conductivity of the composite electrode and this enhances their capacitive performance, which is in accordance to the results obtained from the CV measurement. This decrease in ESR resulted in the increase

in power density for the composite electrodes. The cyclic stability of the electrode material is a crucial and important parameter to rank the performance of the energy storage application [3], [13]. The electrochemical stability of the composites electrodes was evaluated by repeating the CV test between 0.0 and 1.3 V at a scan rate of 100 mV/s for 1000 cycles under the same condition of the electrochemical set-up applied for one cycle. The composites electrode showed a greatly improved cycling stability and demonstrated the positive synergistic effect of AgxSnO1-x ($0.3 \leq x \leq 0.4$) material with the reduce graphene oxide as composite electrode to meet the requirement for high energy and power density. The electrode showed greatly improved cycling stability and demonstrated the positive synergistic effect of AgxSnO1-x ($0.3 \leq x \leq 0.4$) material with the reduce graphene oxide as composite electrode to meet the requirement for high energy and power density. The electrode, AgxSnO1-x/G ($x = 0.4$) after 1000 cycles CV test, gives 117.4 F/g with the capacitance efficiency of 95.4 %. The electrode, AgxSnO1-x ($x = 0.3$) after 1000 cycles CV test, gives 115.5 F/g with the capacitance efficiency of 94.9 % capacitance retention.

CONCLUSION

In summary the reduce graphene oxide (G) was synthesized using the modified Hummer's method and the composite AgxSnO1-x/G ($0.3 \leq x \leq 0.4$) was synthesized using hydrothermal reduction technique. The introduction of AgxSnO1-x ($0.3 \leq x \leq 0.4$) material into the network of the reduce graphene oxide enhances the kinetic for both charge transfer and ion transport throughout the composite electrode. The electrode material takes the advantages of the synergetic effect of the intercalation of the cation doped SnO (AgxSnO1-x) with the reduce graphene oxide (G). The electrode AgxSnO1-x ($x = 0.4$) gives the specific capacitance of 123.1 F/g, energy density of 30.9 Wh/kg and power density of 541.1 W/kg after one cycle and after 1000 cycles CV test, it gives the capacitance efficiency of 95.4 % capacitance retention. The electrode AgxSnO1-x ($x=0.3$) gives the specific capacitance of 121.7 F/g, energy density of 29.3 Wh/kg and power density of 394.6 W/kg after one cycle and after 1000 cycles CV test, it gives the capacitance efficiency of 94.9 %. The composites showed greatly improved cycling stability and revealed the positive synergistic effect of AgxSnO1-x ($0.3 \leq x \leq 0.4$) material with the reduce graphene oxide as composite electrode to meet the requirement for high energy and power density.

Acknowledgement

REFERENCES

Ali, S.M., Muhammad, J., Hussain, S.T., Bakar, S.A., Ashraf, M., and Naeem, U.R. (2013) Study of microstructural, optical and electrical properties of Mg dopped SnO thin films. Journal of Materials Science: Materials in Electronics; 24, pp. 2432–2437.

Augustyn, V., Come, J., Lowe, M.A., Kim, J.W., Taberna, P.L., Tolbert, S.H., Abruna, H.D., Simon, P., and Dunn, B. (2013). Psuedocapacitor oxide materials for high-rate electrochemical energy storage.Nature Materials. 12, pp. 518.

Beguin, F., Presser, V., Balducci, A., and Frackowiat, E.(2014). Carbon and electrolytes Foradvance supercapacitor.Advance matter. 2219, pp. 26-28.

Bello, A., Barzegar, F., Momodu, D., Dangbegnon, J., Taghizadeh, F., and Manyala, N. (2015) Symetric supercapacitor based on porous 3D interconnected Carbon framework. Electrochim Acta. 386 pp.151.

Bidhan, P., Sanjay R. D., Bhanu P. S. and Babasaheb R. S. (2017). Free-standing flexible MWCNTs bucky paper: Extremely stable and energy efficient supercapacitive electrode.Electrochimica Acta, 249, pp.395-403.

Conway, B. (1999). Electrochemical Supercapacitors: Scientific Fundamentals and Technological Applications, Kluwer Academic Publishers, Plenum Press: New York, New York.

Gao, Z., Wang, J., Li, Z., Yang, W., and Wang, B. (2011). Graphene nanosheet/NiAl layered double Hydroxide composite as a novel electrode for a supercapacitor. Chemical mater. 32, pp.3509.

Hoai, P. P.,Thanh, G. L., Quang, T. T.,Hoang H. N., Huynh, T. H., Hoang, T. T. and Tran V. C. (2017) Characterization of Ag-Doped P-Type SnO Thin Films Prepared by DC Magnetron Sputtering.Journal of Nanomaterials. 34, pp. 234-337.

Hsu, P.C., Chen, W.C. and Tsai, Y.T. (2013). Fabrication of p-typeSnO thin-film transistors by sputtering with practical metal electrodes. Japanese Journal of Applied Physics. 52(5), pp. 232-23.

Junfu, L., James, O., Xianghui, H. and George Z. C. (2017). Faradaic processes beyond Nernst's Law, densityfunctional theory assisted modelling of partial electron delocalisation and pseudocapacitance in graphene oxides. Chemistry Communication. 53, pp.10414.

Largeot, C., Portet, C., Chmiola, J., Taberna, P.L., Gogotsi, Y., and Simon, P. (2008) Confinement, desolvation and electrosorption effects on the diffusion of ions in nanoporous carbon electrode.Journal of American Chemical Society. 130, pp. 2730.

Lowsk, A.K., Cki, J.C., and Beker, B. (2008). Influence of grain size on deformation mechanism: an extension to nanocrystalline materials. Dalton Ttransactions.; 47, pp. 6825.

Madhu, C., Bose, V.C., Maniammal, A.S., Aiswarya, A.S., Biju, V. (2014). Effect of aging on nanostructure nickel oxide samples. BijuPhysica, 421, pp. 87

Martinelli, A., Palenzona, A., Putti, M. and Ferdeghini, C. (2009). Microstructural transition in 1111 Oxy-Pnictides. J.W.Lynn, Pengcheng Dai Physica.; C469.

Nakazawa, K., Itoh, S., Matsunaga, T., Matsukawa Y., Satoh, Y and Abe, H. (2014). Effect of dislocation and grain boundary on deformation mechanism in ultrafine- graine interstitial- free steel. Material Science and Engineering. 63, pp. 012125.

Ozolin, V., Zhou F., and Asta, M. (2013). Account of Chemical Research., 46: pp.1084-1093.

Pandolfo, A.G., and Hollenkamp, A.F. (2006). Carbon properties and their role insupercapacitors. Journal of Power Sources.; 11, pp.157-160.

Pandolfo, A.G., and Hollenkamp, A.F.(2006). Carbon properties and their role in supercapacitors. Journal of Power Sources; 11: pp.157-160.

Raymundo-Pinero, E., Kierzek, J., Lota, G., Gryglewicz, G., and Machnikowski, J. (2004). Electrochemical capacitor based on highly porous carbons prepared by KOH activator.Electrochim Acta. 515, pp.49-52.

Siamak, P.J., Alagarsamy, P., Boon, T.G., Hong, N.L. and Nay, M.H. (2015). Influence of particle size on performance of Nickel nanoparticles-based supercapacitor. RSC Advances. 5, pp.14010-14019.

Uwe, H., and Neil, G. (2011). The Scherrer equation versus the Debye-Scherrer equation Nature Nanotechnology. 6, pp. 534.

Yang, Q., Lu, Z., Liu, J., Lei, X., Chang, Z., Luo, L., & Sun, X. Ultrathin Co3O4 nanosheet arrays with high supercapacitive performance. Progress in Natural ScienceMaterials International. 23, pp.1-7.